

## The semi-infinite spin-3/2 Blume-Capel model

This article has been downloaded from IOPscience. Please scroll down to see the full text article.

1999 J. Phys.: Condens. Matter 11 6147

(<http://iopscience.iop.org/0953-8984/11/32/306>)

View [the table of contents for this issue](#), or go to the [journal homepage](#) for more

Download details:

IP Address: 171.66.16.220

The article was downloaded on 15/05/2010 at 16:58

Please note that [terms and conditions apply](#).

## The semi-infinite spin-3/2 Blume–Capel model

A Bakchich<sup>†</sup> and M El Bouziani<sup>‡</sup>

<sup>†</sup> Département de Physique, Faculté des Sciences, BP 4010, Meknès, Morocco

<sup>‡</sup> Laboratoire de Physique de la Matière Condensée, Faculté des Sciences, BP 20, El Jadida, Morocco

Received 6 January 1999, in final form 13 April 1999

**Abstract.** As a function of the ratio  $R$  of bulk and surface interactions and the ratio  $D$  of bulk and surface crystal field we have determined, within the framework both of the mean-field approximation and by renormalization-group techniques, various types of phase diagram of a three-dimensional semi-infinite ferromagnetic spin-3/2 Blume–Capel model. We found that there exist four main types of phase diagram showing a variety of phase transitions associated with the surface and unusual multicritical topologies, including ordinary, extraordinary, surface and special phase transitions. Moreover, in the  $(R, D)$  plane, we determined the domains in which the system exhibits a particular type of phase diagram.

### 1. Introduction

Surface magnetism is an interesting problem which has been the subject of numerous theoretical and experimental studies. Detailed review articles containing an extensive list of references have been published by Binder [1] and Diehl [2]. Most works have been devoted to systems which undergo second-order phase transitions. A relatively small number of papers have considered semi-infinite systems exhibiting first-order and tricritical phase transitions. Of particular interest is the spin-1 Ising model with bilinear and biquadratic nearest-neighbour pair interactions and a single-ion potential, known as the Blume–Emery–Griffiths (BEG) model [3]. The model with vanishing biquadratic interactions is called the Blume–Capel (BC) model [4, 5]. If such systems are bounded by a surface, the local critical and tricritical behaviours are modified in the vicinity of that surface. Those semi-infinite systems have not been studied as extensively as the pure systems, and the theory of surface magnetism seems to be far from complete, although some progress has been noted recently [6, 7].

An extension of the BEG and BC models is the possibility of inclusion of higher spin values. The spin-3/2 BEG model was initially introduced in connection with experimental results on magnetic and crystallographic phase transitions in some rare-earth compounds such as  $\text{DyVO}_4$ , and then extended to describe tricritical properties in ternary fluid mixtures. It has been analysed using a variety of approximations and mathematical techniques, including the mean-field approximation (MFA) [8, 9], real-space renormalization-group (RSRG) calculations [10] and Monte Carlo simulations [9]. Almost no attempts are available in the literature concerning the most interesting problem where we have to consider this model on semi-infinite lattices, with different couplings at the surface and in the bulk. It is our purpose to perform such a study and to check whether such systems can exhibit surface magnetism. Using the MFA and an RSRG method based on the Migdal–Kadanoff (MK) [11, 12] recursion relations, we study the criticality associated with the spin-3/2 BC model on a semi-infinite three-dimensional

hypercubic lattice. As in the case of the spin-1/2 Ising model, we have shown four different types of phase transition associated with the surface, which can be designated using the same known terminology [13, 14], namely, the ordinary transition with simultaneous onset of bulk and surface order, the surface transition where the surface orders first, the subsequent extraordinary transition where the bulk orders in the presence of an already ordered surface and the special transition with bulk and surface ordering at the same temperature but with a different set of critical exponents.

According to the values of the ratio  $R$  of bulk and surface interactions and the ratio  $D$  of bulk and surface crystal fields, we have determined various types of phase diagram featuring a variety of phase transitions associated with the surface, with critical and special transition points. However, our analysis has led to a classification scheme with four fundamental types of phase diagram some of which we have illustrated in the  $(J_S^{-1}, \Delta_S J_S^{-1})$  plane, where the subscript  $S$  refers to the surface. Finally in the  $(R, D)$  plane we have determined the domains in which the system exhibits a particular type of phase diagram.

The present paper is organized as follows. In section 2 we present qualitative phase diagrams of the three-dimensional model determined within the MFA. Quantitative results obtained from an RSRG method are shown in section 3. Finally we draw our conclusion in section 4.

## 2. Mean-field phase diagrams

The three-dimensional cubic spin-3/2 BC model is described by the reduced Hamiltonian

$$-\beta H = J \sum_{\langle ij \rangle} S_i S_j + \Delta \sum_i S_i^2 \quad (1)$$

where each spin variable  $S_i$  takes on the values  $\pm 3/2$  and  $\pm 1/2$ , and  $J$  (positive, since we study the ferromagnetic case) is the reduced coupling constant between neighbouring spins and  $\Delta$  the reduced crystal-field known to exhibit tricritical behaviour.

The different phases of the model described by the Hamiltonian (1) can be characterized by two parameters: the magnetization  $m = \langle S_i \rangle$  and the quadrupole parameter  $q = \langle S_i^2 \rangle$ . According to the values of  $m$  and  $q$  the model has three different phases, and in the plane  $(J^{-1}, \Delta J^{-1})$  its phase diagram, determined within the MFA, is shown in figure 1. It is divided by transition lines into three regions. Two of these are occupied by ferromagnetic phases characterized by  $m \neq 0$ : one (labelled  $F_{3/2}$ ) has large quadrupole order parameter  $q$ , the other ( $F_{1/2}$ ) has small  $q$ . These distinct dense and dilute versions of the ordered phase are separated by a first-order transition line which terminates at a critical point (C), instead of the tricritical point obtained previously [9]. In the remaining region, the paramagnetic ( $m = 0$ ) phase (P) occurs, which is separated from the ferromagnetic phases by a single second-order transition line.

In this paper we shall consider the three-dimensional semi-infinite cubic spin-3/2 BC model described by the reduced Hamiltonian

$$-\beta H = J_S \sum_{\langle ij \rangle} S_i S_j + \Delta_S \sum_i S_i^2 + J_B \sum_{\langle kl \rangle} S_k S_l + \Delta_B \sum_k S_k^2 \quad (2)$$

where  $J_S$  is the reduced coupling constant between neighbouring spins located on the two-dimensional surface of the system, and  $J_B$  is the reduced coupling constant between remaining neighbouring spins, which is not necessary equal to the surface one  $J_S$ , and  $\Delta_S$  and  $\Delta_B$  are reduced crystal-fields respectively at the surface and in the bulk.

If we denote respectively by  $m_S, m_B, q_S$  and  $q_B$  the surface and the bulk magnetizations and quadrupole momenta per site, a straightforward calculation leads to the following mean-field

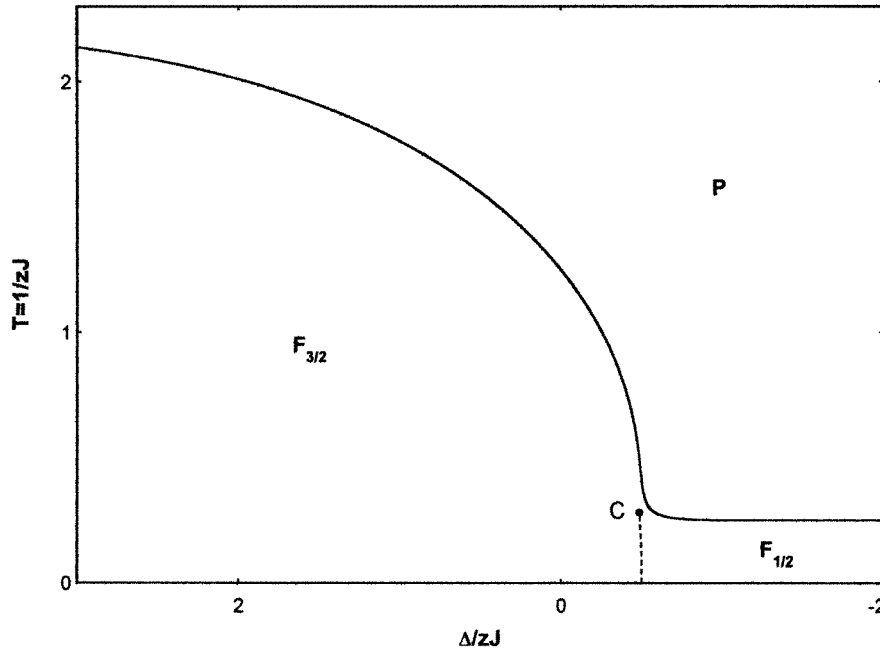


**Figure 1.** Phase diagram of the three-dimensional spin-3/2 Blume–Capel model determined within the mean-field approximation. Solid and dashed lines, respectively, indicate second- and first-order phase transitions. The symbols P and F refer to the paramagnetic and ferromagnetic phases. C is a critical point.

equations:

$$m_\alpha = \frac{\frac{1}{2} e^{\frac{1}{4}\Delta_\alpha} \sinh\left(\frac{1}{2}M_\alpha\right) + \frac{3}{2} e^{\frac{9}{4}\Delta_\alpha} \sinh\left(\frac{3}{2}M_\alpha\right)}{e^{\frac{1}{4}\Delta_\alpha} \cosh\left(\frac{1}{2}M_\alpha\right) + e^{\frac{9}{4}\Delta_\alpha} \cosh\left(\frac{3}{2}M_\alpha\right)} \quad (3)$$

$$q_\alpha = \frac{\frac{1}{4} e^{\frac{1}{4}\Delta_\alpha} \cosh\left(\frac{1}{2}M_\alpha\right) + \frac{9}{4} e^{\frac{9}{4}\Delta_\alpha} \cosh\left(\frac{3}{2}M_\alpha\right)}{e^{\frac{1}{4}\Delta_\alpha} \cosh\left(\frac{1}{2}M_\alpha\right) + e^{\frac{9}{4}\Delta_\alpha} \cosh\left(\frac{3}{2}M_\alpha\right)}$$

where  $\alpha = B$  or  $S$  refers to the bulk or the surface, and

$$M_B = z_B J_B m_B$$

$$M_S = z_S J_S m_S + J_B m_B$$

with  $z_S$  and  $z_B$  the coordination numbers on the surface and in the bulk of the lattice.

The bulk and surface free energies per site of the semi-infinite system can be written as

$$\frac{F_B}{T} = -\ln \left[ 2 e^{\frac{1}{4}\Delta_B} \cosh\left(\frac{1}{2}M_B\right) + 2 e^{\frac{9}{4}\Delta_B} \cosh\left(\frac{3}{2}M_B\right) \right] + \frac{z_B}{2} J_B m_B^2 \quad (4)$$

$$\frac{F_S}{T} = -\ln \left[ 2 e^{\frac{1}{4}\Delta_S} \cosh\left(\frac{1}{2}M_S\right) + 2 e^{\frac{9}{4}\Delta_S} \cosh\left(\frac{3}{2}M_S\right) \right] + \frac{z_S}{2} J_S m_S^2 + \frac{(z_B - z_S)}{2} J_B m_B^2. \quad (5)$$

The self-consistent equations (3) are solved numerically. The solution which minimizes the free energy represents the stable equilibrium phase. If there are two solutions which have the same minimum free energy, these phases coexist and the system has a first-order phase transition.

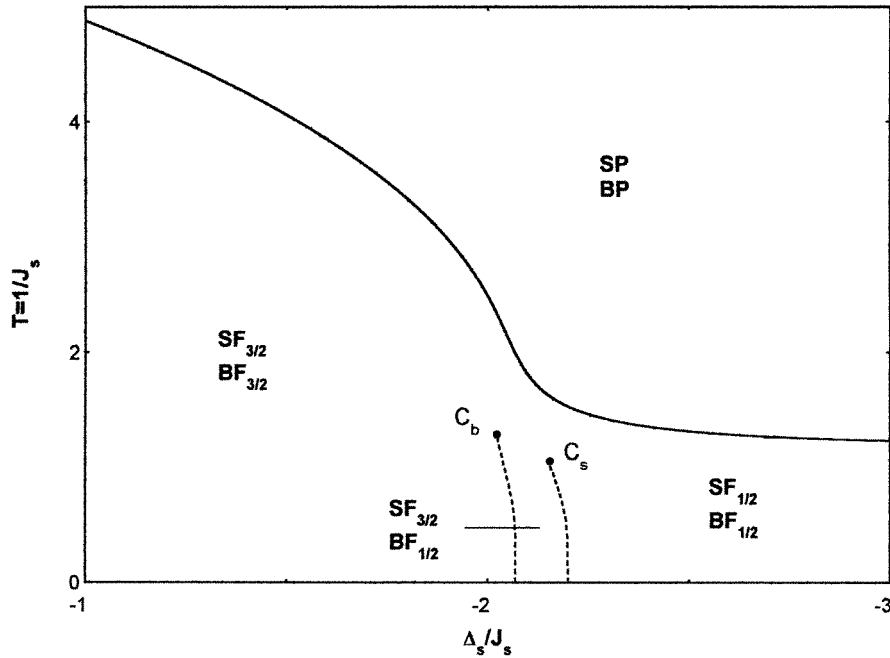


**Figure 2.** Type 1 phase diagram for the three-dimensional semi-infinite spin-3/2 Blume–Capel model calculated in the mean-field approximation with  $R = 0.8$  and  $D = 1.16$ . The symbols SP, BP, SF and BF denote, respectively, surface paramagnetic, bulk paramagnetic, surface ferromagnetic and bulk ferromagnetic phases.  $C_S$  and  $C_B$  characterize two critical points on the surface and in the bulk, respectively.

For the semi-infinite BC model we define the ratios  $R = J_B/J_S$  and  $D = \Delta_B/\Delta_S$  and classify the possible phase diagrams illustrated in the  $(J_S^{-1}, \Delta_S J_S^{-1})$  plane at fixed  $R$  and  $D$ . The mean-field analysis that has been undertaken suggests qualitatively interesting features of the model. However, our analysis has led to a classification scheme with four fundamental types of phase diagram showing ordinary, extraordinary, surface and special phase transitions. The nature of the surface and bulk order is indicated in each region by the symbols P for paramagnetic and  $F_{3/2}$  or  $F_{1/2}$  for ferromagnetic phases, preceded by the symbols B for bulk and S for surface. Second-order and first-order parts of the phase boundary are shown as full and dashed lines, respectively.

According to the values of the ratios  $R$  and  $D$ , different qualitative types of phase diagram are expected. To classify them we shall proceed as follows:

(1) *Type 1.* The system exhibits only ordinary phase transitions of second-order between different phases  $F_{3/2}$ ,  $F_{1/2}$  and P. We have also shown unusual successive phase transitions of first order, where the surface and the bulk of the system exhibit a transition between the two ordered phases  $F_{3/2}$  and  $F_{1/2}$ , terminating at two critical points  $C_S$  and  $C_B$  associated with the surface and the bulk, respectively. According to the position of the critical points, three different cases can be distinguished: (a) the transition between the ferromagnetic phases on the surface ( $SF_{3/2} \leftrightarrow SF_{1/2}$ ) is realized before the one in the bulk ( $BF_{3/2} \leftrightarrow BF_{1/2}$ ). Thus the surface transition line terminated at the critical point  $C_S$  is inside the ferromagnetic phase  $BF_{3/2}$ . (b) The surface transition line ( $SF_{3/2} \leftrightarrow SF_{1/2}$ ) is realized inside the ferromagnetic phase  $BF_{1/2}$ . (c) In between these two topologies, a limit phase diagram occurs, where the

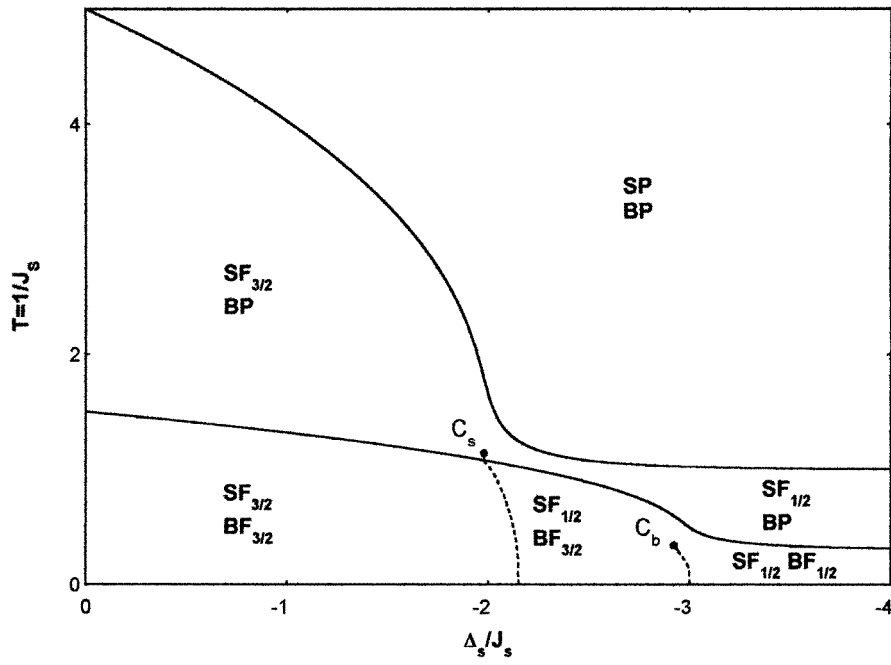


Figure 3. A type 2 phase diagram from the global mean-field approximation calculated for  $R = 0.2$  and  $D = 0.2$ .

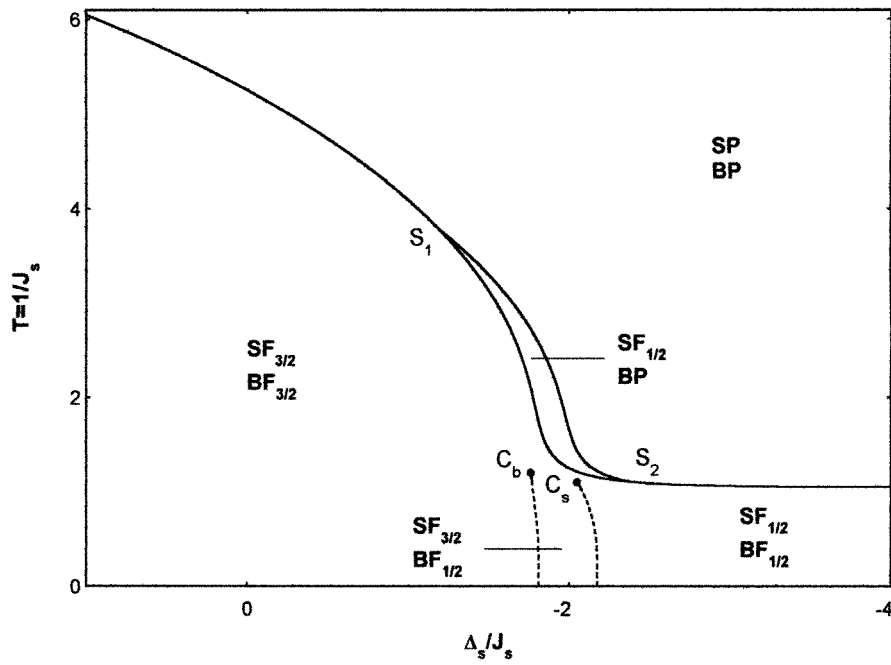


Figure 4. A type 3 phase diagram calculated for  $R = 0.7$  and  $D = 1.16$ .

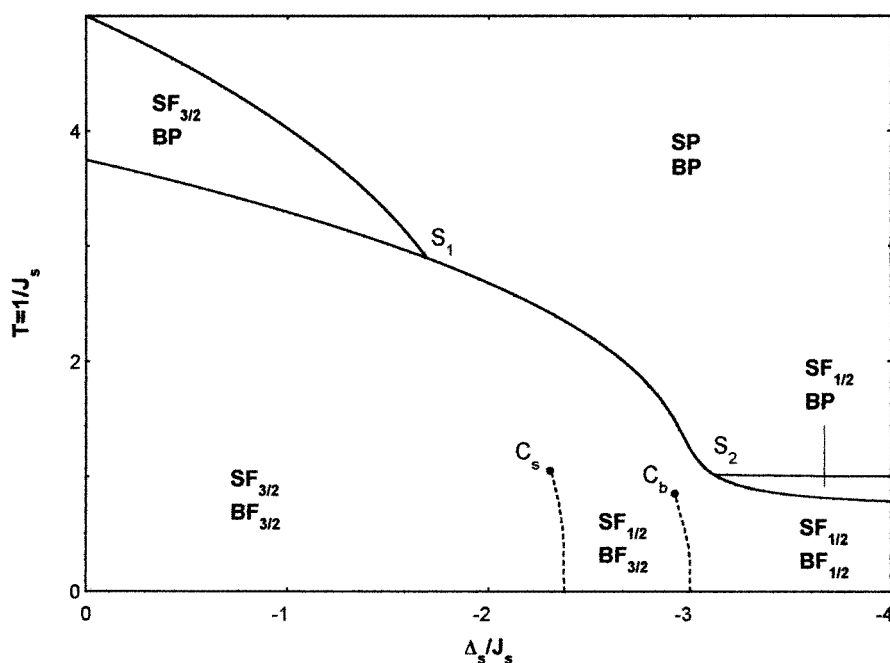


Figure 5. A type 4 phase diagram calculated for  $R = 0.5$  and  $D = 0.5$ .

first-order transitions on the surface and in the bulk between the two ferromagnetic phases are simultaneous. A typical phase diagram showing the various phase transitions is represented in figure 2.

(2) *Type 2.* As a function of the ratios  $R$  and  $D$ , different types of phase diagram have been found. We have shown extraordinary and surface phase transitions of second order. As previously three cases can be distinguished depending on the position of the first-order transition lines separating the two ordered phases on the surface and in the bulk. Figure 3 represents a typical phase diagram.

(3) *Type 3.* According to the values of the ratios  $R$  and  $D$  we have indicated in figure 4 a typical phase diagram among three qualitative types which have been determined. We have shown ordinary, extraordinary and surface phase transitions of second order. Besides these transitions we can observe the successive phase transitions of first order between the two ordered phases. For two particular values of  $\Delta_s/J_s$  there exist two special points ( $S_1$  and  $S_2$ ) characterizing the special phase transition, where a second-order transition line meets two second-order transition lines, particularly a line of extraordinary and surface transitions. At these special points the surface and the bulk of the system become ordered simultaneously.

(4) *Type 4.* As a function of the ratios  $R$  and  $D$ , we obtain three main qualitative types of phase diagrams; one of them is reported in figure 5. It shows ordinary, extraordinary and surface phase transitions of second order. The three transition lines meet at two special phase transition points ( $S_1$  and  $S_2$ ).

### 3. Renormalization-group phase diagrams

In the preceding section we have presented phase diagrams obtained from the MFA to understand qualitative features of the phase transitions of the model. By contrast, in this

section we discuss renormalization-group results obtained from an RSRG transformation, in comparison with the mean-field results. This technique is based on the MK bond-moving approximation which consists of first performing the decimation and then moving the bonds. In what follows, we shall only give a brief description of the method.

Choose a scale factor  $b$  and consider a one-dimensional chain of  $(b + 1)$  spins coupled by nearest-neighbour interactions all equal to  $J$  and a crystal field  $\Delta$ . Perform the trace over all spins on the chain except those at the end. The end spins are then coupled by the effective interactions  $\tilde{J}$  and  $\tilde{\Delta}$ , which are functions of  $J$  and  $\Delta$ .

In an infinite  $d$ -dimensional cubic lattice Migdal argues that the renormalization-group transformations that give the new coupling constant  $J'$  and  $\Delta'$  as a function of  $J$  and  $\Delta$  are simply

$$\begin{aligned} J' &= b^{d-1} \tilde{J}(J, \Delta) \\ \Delta' &= b^{d-1} \tilde{\Delta}(J, \Delta). \end{aligned}$$

In the case of a semi-infinite  $d$ -dimensional cubic spin-3/2 BC model described by the Hamiltonian (2) it is straightforward to extend Migdal's approximate recursion relations [15, 16]. We have

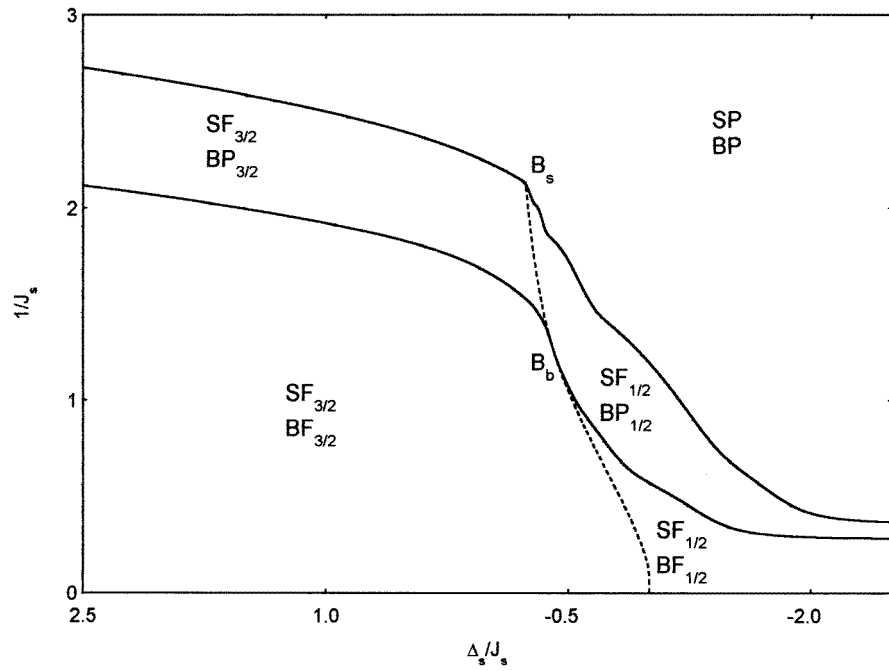
$$\begin{aligned} J'_B &= b^{d-1} \tilde{J}(J_B, \Delta_B) \\ \Delta'_B &= b^{d-1} \tilde{\Delta}(J_B, \Delta_B) \\ J'_S &= b^{d-2} \tilde{J}(J_S, \Delta_S) + \frac{1}{2}(b-1)b^{d-2} \tilde{J}(J_B, \Delta_B) \\ \Delta'_S &= b^{d-2} \tilde{\Delta}(J_S, \Delta_S) + \frac{1}{2}(b-1)b^{d-2} \tilde{\Delta}(J_B, \Delta_B). \end{aligned}$$

The renormalization-group phase diagrams are derived from the global study of flows in Hamiltonian space, which are governed by fixed points. The various fixed points underlying the structure of the semi-infinite system have been determined and classified, yielding first-order phase boundaries, critical, tricritical and multicritical points (we used the Nienhuis–Nauenberg criterion [17] for seeing first-order transitions in the RSRG method).

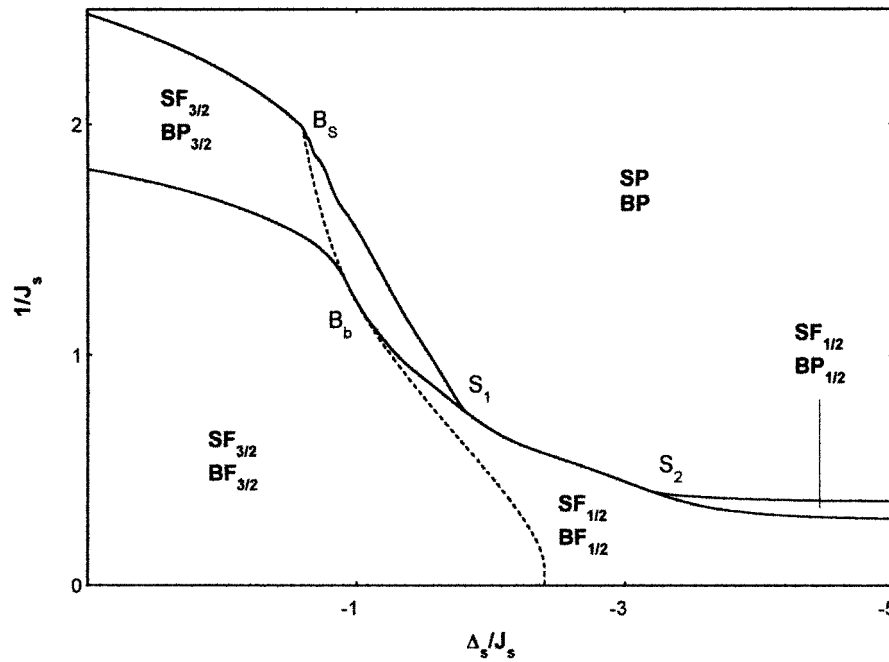
Using renormalization-group calculations, we have obtained four generic types of phase diagram, illustrated in the  $(J_S^{-1}, \Delta_S J_S^{-1})$  plane for several values of  $R$  and  $D$ , reported in figures 6(a)–(d). They show a variety of phase transitions associated with the surface and unusual multicritical topologies, including certain types of ordinary, extraordinary and special phase transition. To classify the different types of phase diagram, we shall proceed as follows:

- (a) For  $R = 1.2$  and  $D = 0.4$ , the corresponding phase diagram is characterized by extraordinary and surface second-order phase transitions. Moreover, the unusual feature of this phase diagram is the presence of two bicritical points  $B_S$  and  $B_B$ , respectively on the surface and in the bulk, terminating the successive phase transitions of first order between the two ordered phases.
- (b) For  $R = 0.4$  and  $D = 0.5$ , we have shown ordinary, extraordinary and surface phase transitions of second order. According to the values of  $\Delta_S/J_S$ , we can observe two multicritical points  $S_1$  and  $S_2$  characterizing the special phase transitions, in addition to the bicritical points  $B_S$  and  $B_B$ .
- (c) For  $R = 0.62$  and  $D = 0.5$ , the system exhibits phase transitions between different phases as indicated above, with the two special transition points  $S_1$  and  $S_2$ . The two bicritical points occurring in figures (a) and (b) merge into a single bicritical point  $B$ .
- (d) For  $R = 1.0$  and  $D = 0.5$ , the system exhibits only an ordinary phase transition of second order with the bicritical point  $B$ .

In this renormalization-group calculation, a qualitatively different sequence of phase diagrams occurs, but these diagrams are different from the ones of the MFA. The main

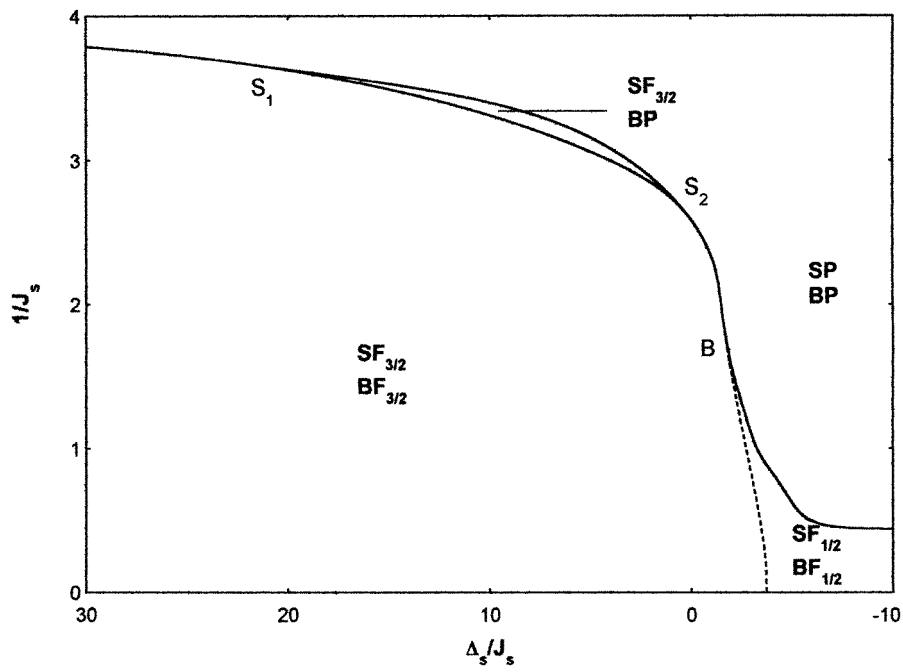


(a)

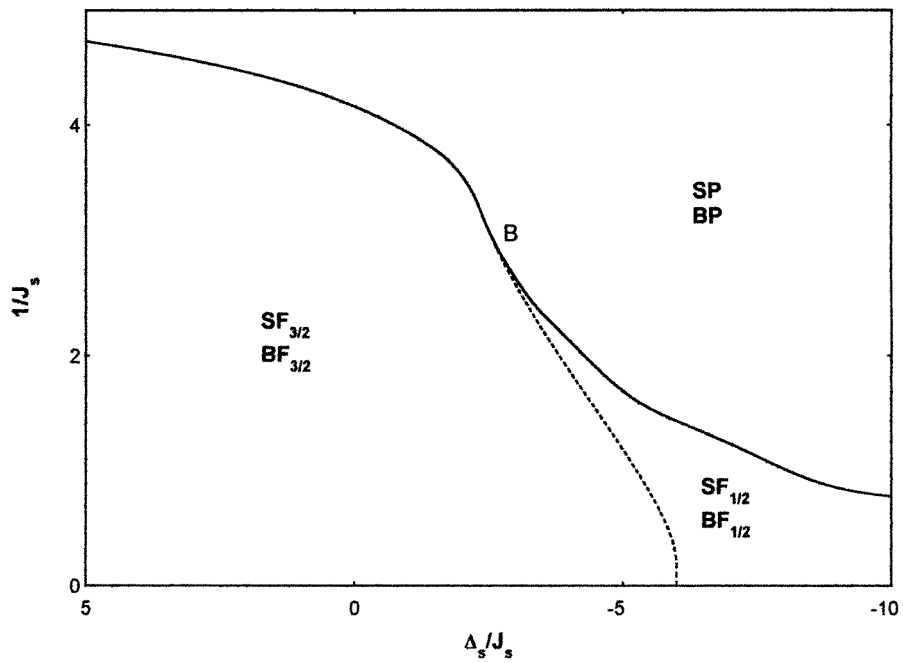


(b)

**Figure 6.** Typical phase diagrams for the three-dimensional semi-infinite BC model, from the global renormalization-group technique, calculated for (a)  $R = 0.3$  and  $D = 0.7$ , (b)  $R = 0.4$  and  $D = 0.5$ , (c)  $R = 0.62$  and  $D = 0.5$ , (d)  $R = 1.0$ ,  $D = 0.5$ .



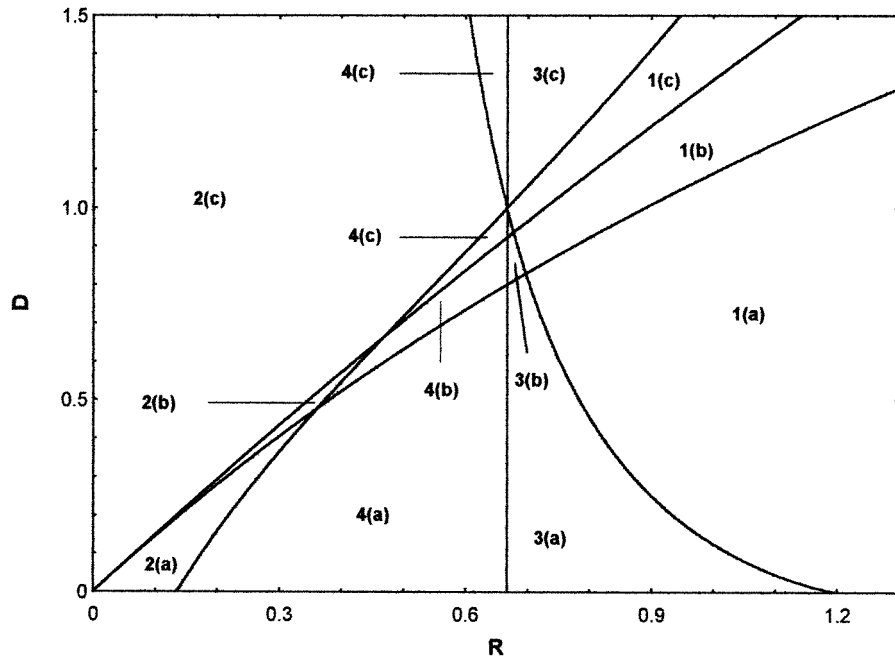
(c)



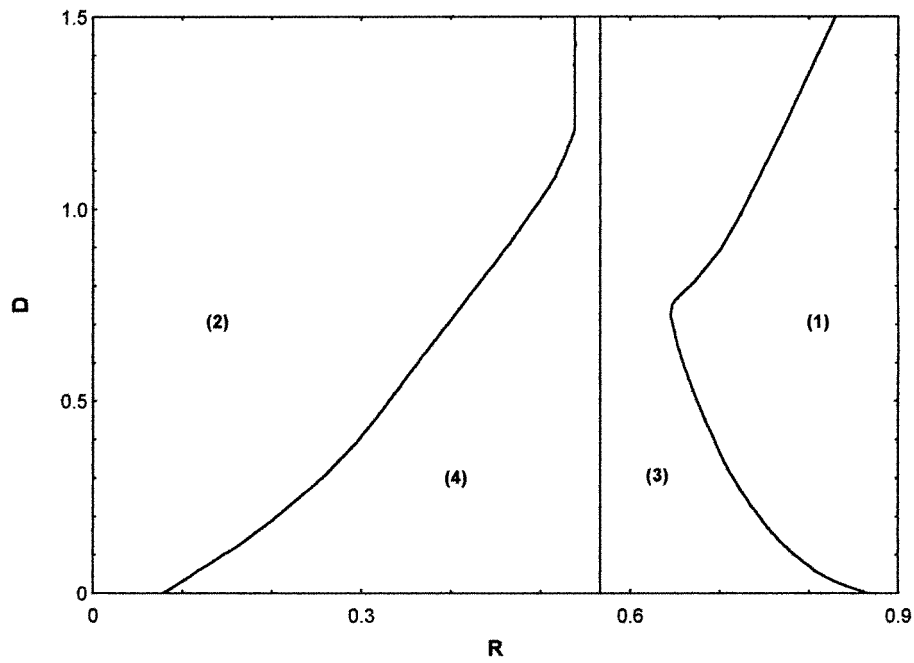
(d)

Figure 6. (Continued)

discrepancy is that no critical points, terminating the first-order transition lines into the ordered phase, are seen. However, the RSRG shows the presence of two bicritical points  $B_S$  and  $B_B$  instead of the critical points  $C_S$  and  $C_B$ .



(a)



(b)

**Figure 7.** Domain of existence of the different types of phase diagram (a) from the mean-field approximation, and (b) from the renormalization-group technique.

Finally, according to the values of the parameters  $R$  and  $D$  we have indicated in figures 7(a) and (b) the domains of existence of the different types of phase diagram which have been determined.

#### 4. Conclusion

We have investigated the semi-infinite ferromagnetic spin-3/2 Blume–Capel model, in the framework both of the MFA and by an RSRG technique. Within the two approaches, we have classified the various phase diagrams at fixed  $R$  and  $D$ , finding new types of phase diagram featuring a variety of phase transitions and multicritical points. Finally, we have determined the domains in which the system exhibits a particular type of phase diagram.

#### References

- [1] Binder K 1983 *Phase Transitions and Critical Phenomena* vol 8, ed C Domb and J L Lebowitz (New York: Academic)
- [2] Diehl H W 1986 *Phase Transitions and Critical Phenomena* vol 10, ed C Domb and J L Lebowitz (New York: Academic)
- [3] Blume M, Emery V J and Gruffiths R B 1971 *Phys. Rev. A* **4** 1071
- [4] Blume M 1966 *Phys. Rev.* **141** 517
- [5] Capel H W 1966 *Physica* **32** 966  
Capel H W 1967 *Physica* **33** 295  
Capel H W 1967 *Physica* **37** 423
- [6] Buzano C and Pelizzola A 1993 *Physica A* **195** 197
- [7] Bakchich A and El Bouziani M 1997 *Phys. Rev. B* **56** 11 155  
Bakchich A and El Bouziani M 1997 *Phys. Rev. B* **56** 11 161  
Benyoussef A, Boccara N and El Bouziani M 1986 *Phys. Rev. B* **34** 7775
- [8] Sivardière J and Blume M 1972 *Phys. Rev. B* **5** 1071  
Krinsky S and Mukamel D 1975 *Phys. Rev. B* **11** 399
- [9] Sa Barreto F C and De Alcantara Bonfim O F 1991 *Physica A* **172** 378
- [10] Bakchich A, Bassir A and Benyoussef A 1993 *Physica A* **195** 188
- [11] Migdal A A 1975 *Zh. Eksp. Teor. Fiz.* **69** 1457 (Engl. transl. *Sov. Phys.–JETP* **42** 743)
- [12] Kadanoff L P 1976 *Ann. Phys., NY* **100** 359
- [13] Lubensky T C and Rubin M H 1973 *Phys. Rev. Lett.* **31** 1469  
Lubensky T C and Rubin M H 1975 *Phys. Rev. B* **11** 4533  
Lubensky T C and Rubin M H 1975 *Phys. Rev. B* **12** 3885
- [14] Bray A J and Moore M A 1977 *J. Phys. A: Math. Gen.* **10** 1927
- [15] Lipowsky R and Wagner H 1981 *Z. Phys. B* **42** 355
- [16] Nagai O and Toyonaga M 1986 *J. Phys.: Condens. Matter* **14** L545
- [17] Nienhuis B and Nauenberg M 1975 *Phys. Rev. Lett.* **35** 477